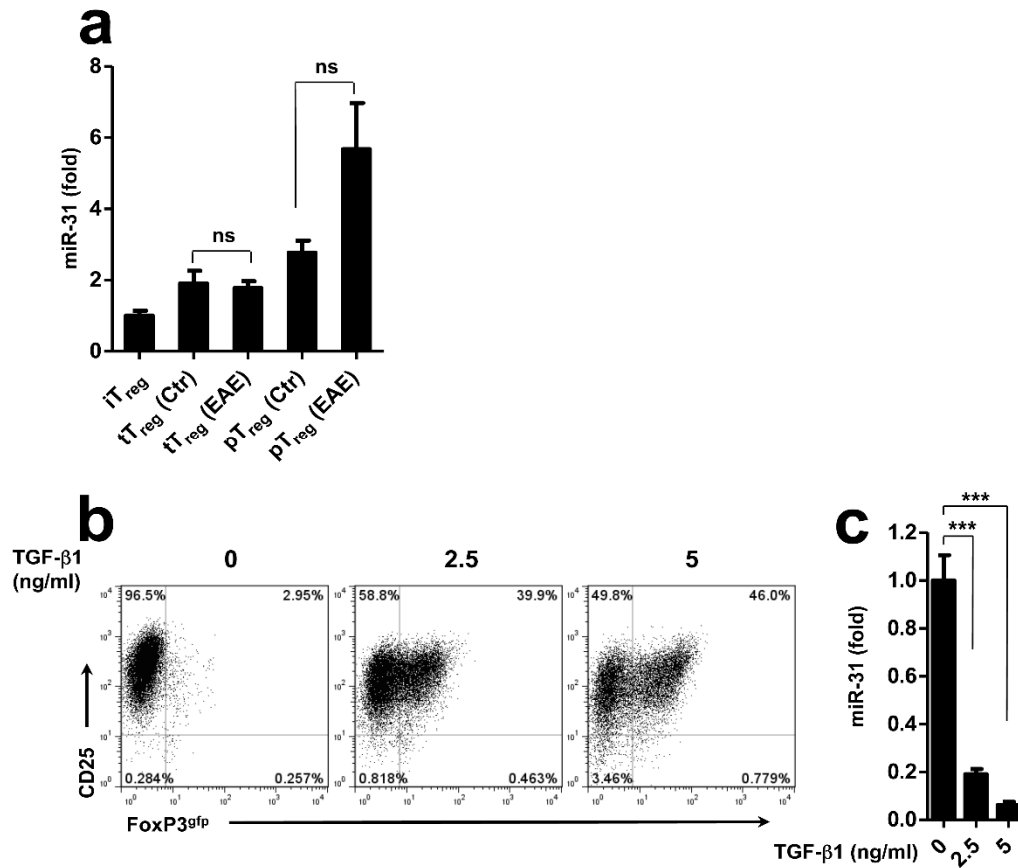
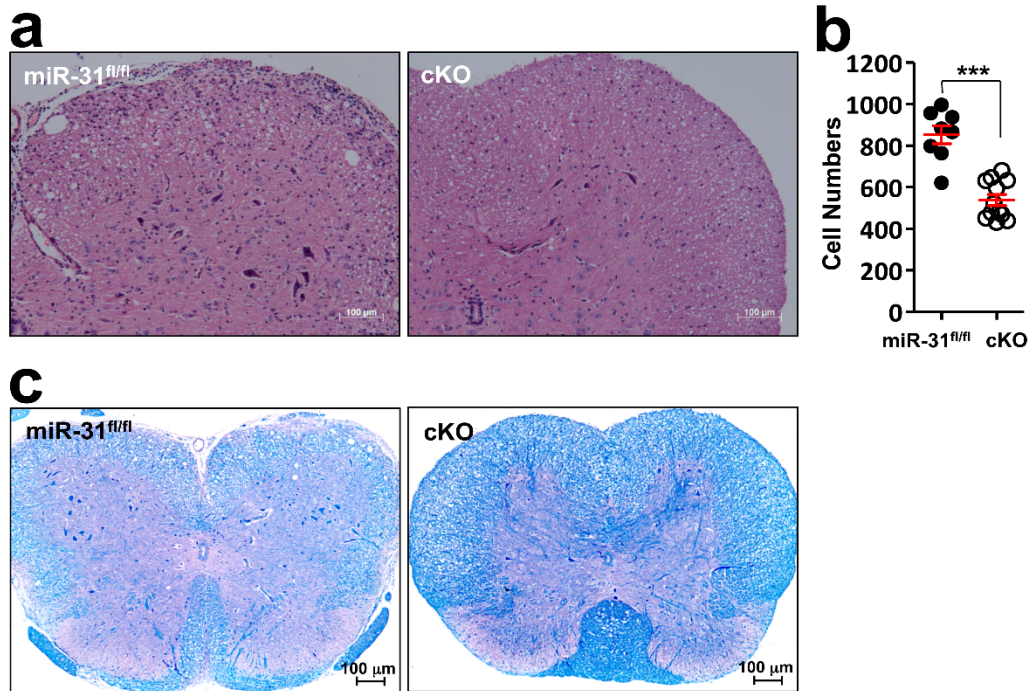


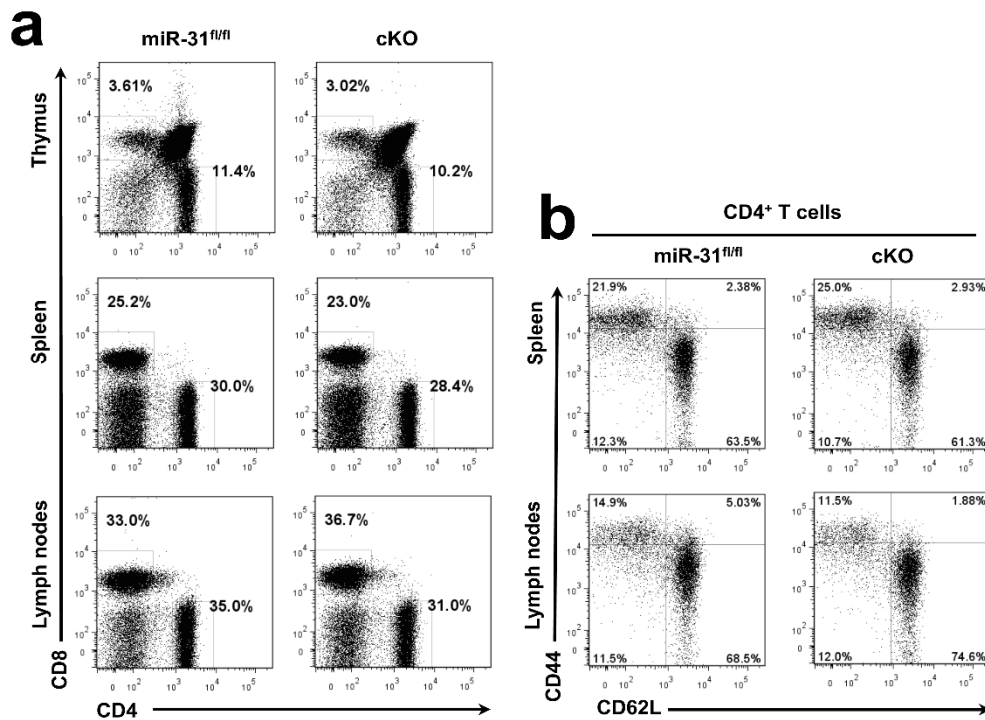
## Supplementary Information



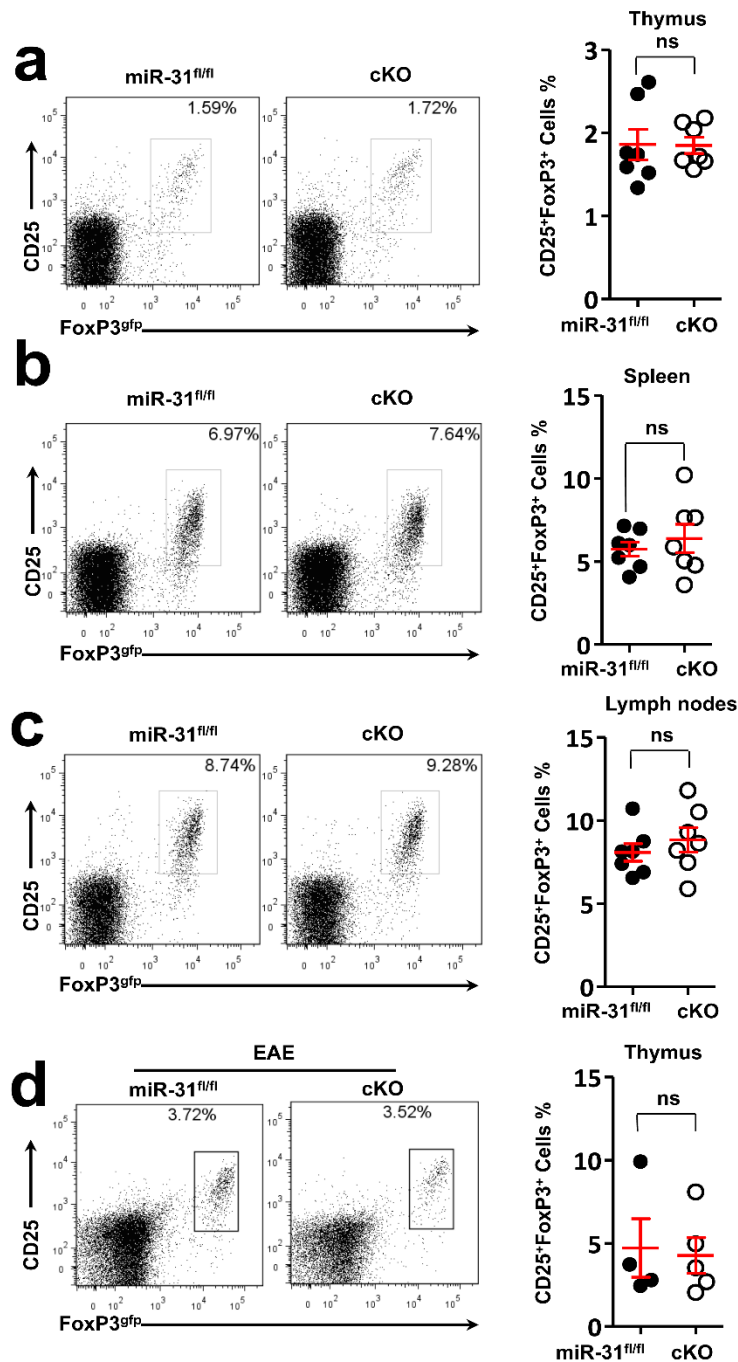
**Supplementary Figure 1 miR-31 expression in T<sub>reg</sub> subsets and its levels are reversely correlated with numbers of iT<sub>reg</sub> cells.** (a) miR-31 expression in iT<sub>reg</sub>, tT<sub>reg</sub>, EAE tT<sub>reg</sub>, pT<sub>reg</sub> and EAE pT<sub>reg</sub> cells; results are presented relative to miR-31 expression in iT<sub>reg</sub> cells. (b) Representative flow cytometry of FoxP3<sup>gfp</sup> expression in iT<sub>reg</sub> cells polarized with different concentrations of TGF-β1. Numbers in quadrants indicate percent cells in each. (c) qPCR analysis of miR-31 expression in iT<sub>reg</sub> cells polarized with different concentrations of TGF-β1; results are presented relative to miR-31 expression in naïve T cells cultured without TGF-β1. ns, not significant, \*\*\**p*<0.001, two-tailed Student's *t*-test. Data are from one experiment representative of two independent experiments (mean ± sem).



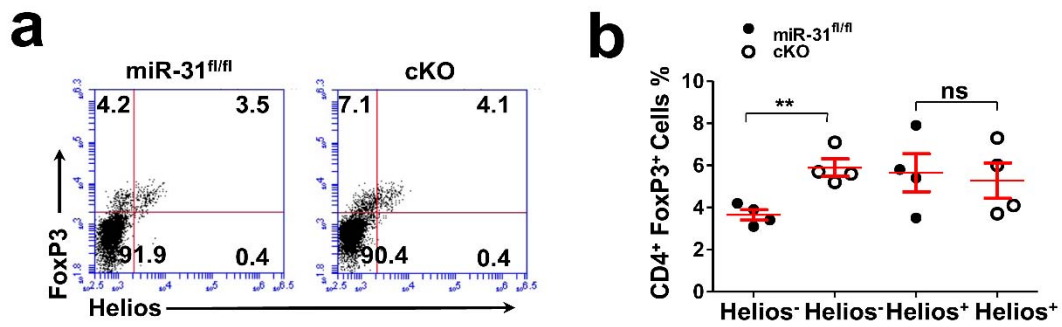
**Supplementary Figure 2 Decreased infiltrating lymphocytes and demyelination of spinal cord in cKO mice with EAE.** (a, b) Infiltrating lymphocytes in the spinal cord of *miR-31<sup>fl/fl</sup>* and cKO mice with EAE were counted. (c) The degree of demyelination of spinal cords from *miR-31<sup>fl/fl</sup>* and cKO mice with EAE was analyzed by Luxol fast blue staining. \*\*\* $p < 0.001$ , two-tailed Student's *t*-test. Representative data are shown, which had been reproduced in two independent experiments.



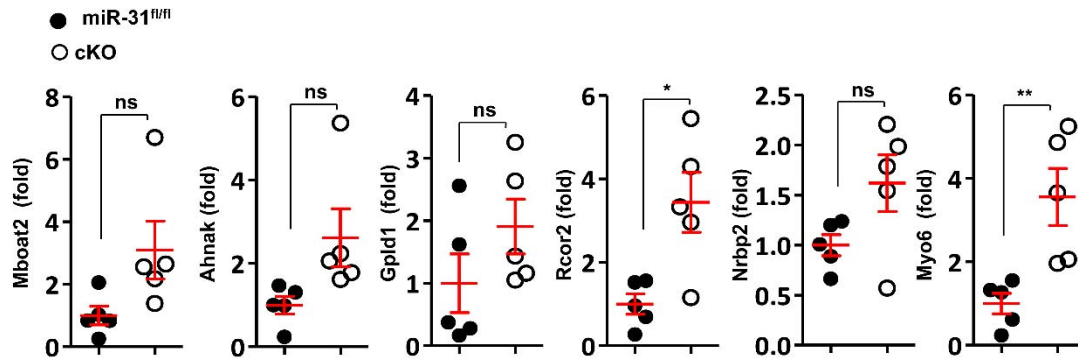
**Supplementary Figure 3 miR-31 deficiency has no apparent effect on the development of T cells.** (a) Representative flow cytometry of CD4<sup>+</sup> and CD8<sup>+</sup> T cells in thymus, spleen and lymph nodes from 6-week old *miR-31<sup>fl/fl</sup>* and cKO mice. (b) Representative flow cytometry for surface expression of CD44 and CD62L in CD4<sup>+</sup> cells in spleen and lymph nodes from 6-week old *miR-31<sup>fl/fl</sup>* and cKO mice. Numbers adjacent to outlined areas or in quadrants indicate percent cells in each. Data are from one experiment representative of two independent experiments.



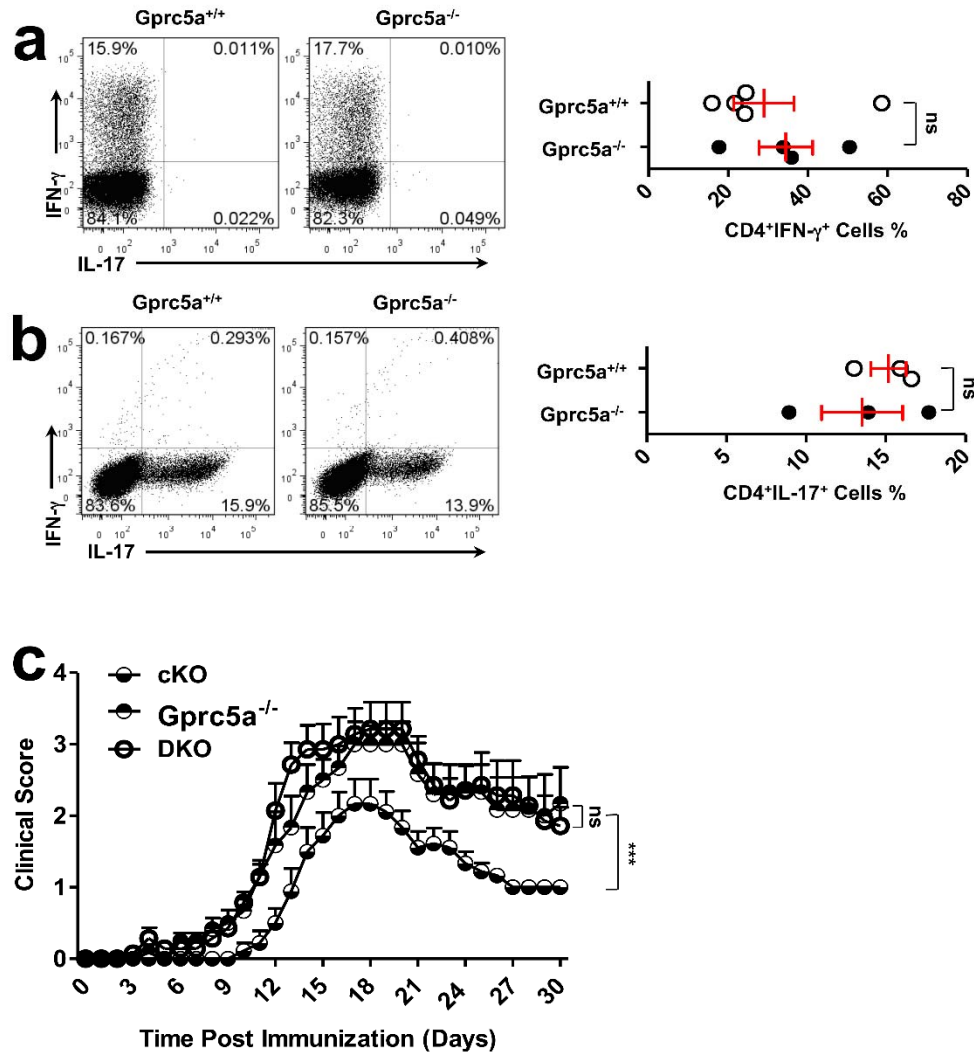
**Supplementary Figure 4 miR-31 deficiency has no impact on tT<sub>reg</sub> cell development.** *FoxP3<sup>gfp</sup>* reporter mice were crossed with either *miR-31<sup>fl/fl</sup>* or *cKO* mice. (a-c) Flow cytometric analysis of T<sub>reg</sub> cells in thymus, spleen and lymph nodes from 6-week old *miR-31<sup>fl/fl</sup>* and *cKO* mice. (d) Flow cytometric analysis of tT<sub>reg</sub> cells in thymus from 6-week old *miR-31<sup>fl/fl</sup>* and *cKO* mice with EAE. Numbers adjacent to outlined areas indicate percent cells in each. ns, not significant, two-tailed Student's *t*-test. Data are representative of three independent experiments (mean ± sem).



**Supplementary Figure 5 Deletion of miR-31 in CD4<sup>+</sup> T cells promotes pT<sub>reg</sub> cell Induction *in vivo*.** Bone marrow cells were prepared from either *miR-31<sup>fl/fl</sup>* or cKO mice. The bone marrow cells ( $5 \times 10^6$ ) were injected intravenously into lethally irradiated C57BL/6J recipient mice to generate bone marrow chimeric mice. Eight weeks after bone marrow transplantation, EAE was induced in all chimeric mice. **(a, b)** Splenocytes prepared from *miR-31<sup>fl/fl</sup>* or cKO chimeric mice 10 days post immunization were subjected for analysis of Helios<sup>-</sup>FoxP3<sup>+</sup> pT<sub>reg</sub> cells and Helios<sup>+</sup>FoxP3<sup>+</sup> nT<sub>reg</sub> cells by Flow cytometry (cells were gated in CD4<sup>+</sup> T cell population). Data are representative of three independent experiments. \*\* $p < 0.01$ , two-tailed *Student's test*.



**Supplementary Figure 6 mRNA levels of candidate genes targeted by miR-31 in iT<sub>reg</sub> cells.** mRNA levels of 6 candidate genes were measured by qPCR. Results are presented as the ratio of mRNA to  $\beta$ -actin, relative to that in *miR-31<sup>fl/fl</sup>* controls. \* $p < 0.05$ , \*\* $p < 0.01$ , ns, not significant, two-tailed Student's *t*-test. Data are representative of two independent experiments (mean  $\pm$  sem).



**Supplementary Figure 7** *Gprc5a* deficiency does not affect  $T_H1$  and  $T_H17$  cell differentiation *in vitro*, but restores the disease phenotype in cKO mice. (a, b) Flow cytometric analysis of  $T_H1$  and  $T_H17$  cells polarized from naïve T cells of either *Gprc5a*<sup>+/+</sup> or *Gprc5a*<sup>-/-</sup> mice (n=3-4). Numbers in quadrants indicate percent cells in each. (c) miR-31 mice were crossed with *Gprc5a*<sup>-/-</sup> mice to generate DKO mice. Clinical scores (mean  $\pm$  sem) of cKO, *Gprc5a*<sup>-/-</sup> and DKO mice after the induction of EAE were assessed every day (n=6-8). \*\*\* $p$ <0.001, ns, not significant, two-tailed Student's *t*-test for (a, b), one-way ANOVA for (c). Data are from one representative of two independent experiments for (a, b) (mean  $\pm$  sem).

**Fig 5.e**

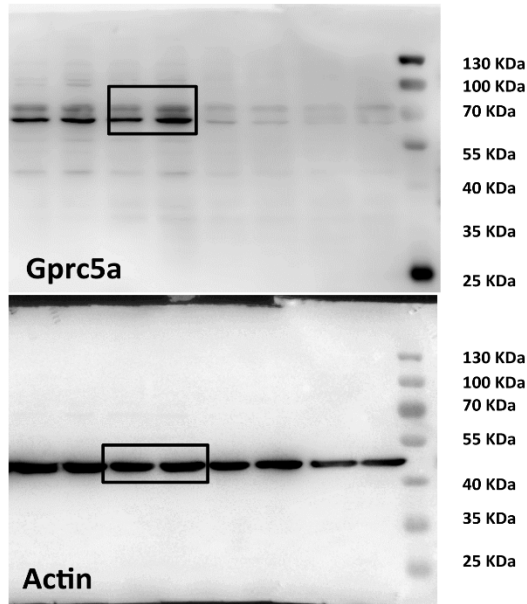


**Fig 6.c**

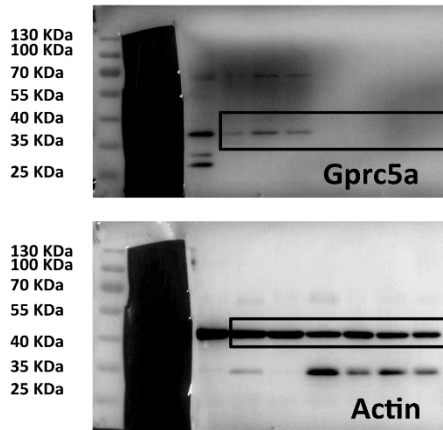
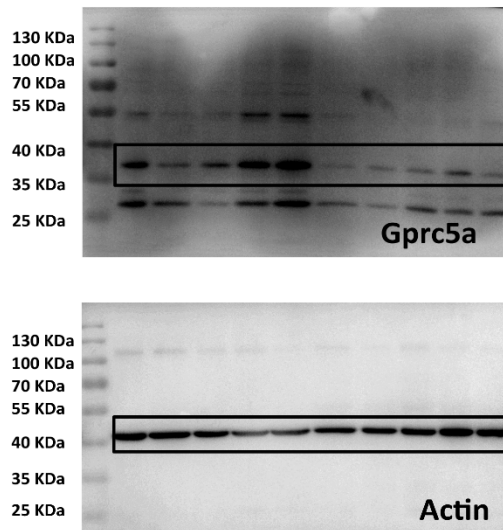


**Fig 6.d**



Supplementary Figure 8 List of original pictures of western blots. Black boxes highlight the indicated lanes in figures.



## Supplementary Table 1

Primers used in this study

<b>Molecule</b>	<b>Primer</b>	<b>Sequence</b>
<b>FoxP3</b>	Upstream	CCCAGGAAAGACAGCAACCTT
	Downstream	TTCTCACAACCAGGCCACTTG
<b>b-actin</b>	Upstream	TGGAATCCTGTGGCATCCATGAAAC
	Downstream	TAAAACGCAGCTCAGTAACAGTCCG
<b>Mboat2</b>	Upstream	TCAGACACGTAGTTGCTACCC
	Downstream	TGCAGTAGGAAATCCCACCTTG
<b>Ahnak</b>	Upstream	CAGCGCATCTACACCACGAA
	Downstream	CACTTCATGCCTTGGTATCTTGA
<b>Gpld1</b>	Upstream	TATTCGAGAGAACTACCTCTGC
	Downstream	AGGAACCCTTGTTCAATACCCA
<b>Rcor2</b>	Upstream	ATCCGAGTTGGAACCAATTACC
	Downstream	AGTGCCTGCTCAATGTTATAGC
<b>Gprc5a</b>	Upstream	ACCACAGACTTTGTGACCTGG
	Downstream	CGAGTGCAAACATGCAAGCC
<b>Myo6</b>	Upstream	CCACAATGTCAAAGTTCGGTACA
	Downstream	GGCATCGTCCCAAGAGATTTTC
<b>Nrbp2</b>	Upstream	AACGGGATCTATCCACTGATGA
	Downstream	GGTCTCCGAGTCAAAGGGTTC
<b>miR-31 -344~458</b>	Upstream	5'-TGCACGGGAGCATTTCATACA
	Downstream	5'-GGATCCAATGGCGTTCAAGC
<b>miR-31 -531~795</b>	Upstream	TCTCCTTTCCCTCACCCCACT
	Downstream	GACATGCGCTTTCCCAATCC
<b>miR-31-1175~1274</b>	Upstream	GTGACATGTTTGACTGCCGA
	Downstream	TGGCTCTGACTCATGAACTCC
<b>miR-31-1800~1936</b>	Upstream	TGTTCCGTTTACAAGCCCAT
	Downstream	AGGCTTTGATCCAGGCAGAC